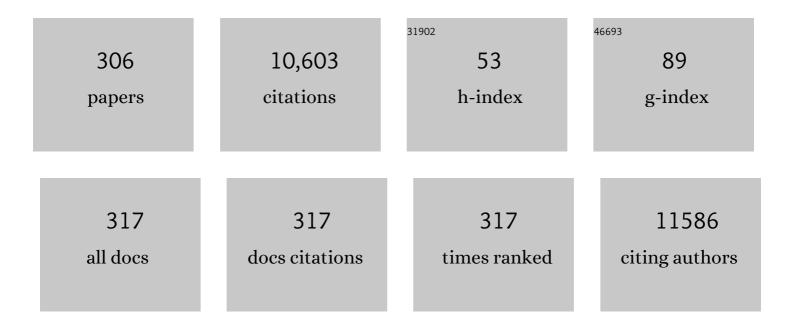
List of Publications by Year in descending order

Source: https://exaly.com/author-pdf/4166462/publications.pdf Version: 2024-02-01



#	Article	IF	CITATIONS
1	Reactive binder and aggregate interfacial zones in the mortar of Tomb of Caecilia Metella concrete, 1C BCE, Rome. Journal of the American Ceramic Society, 2022, 105, 1503-1518.	1.9	10
2	Scaling of the strange-metal scattering in unconventional superconductors. Nature, 2022, 602, 431-436.	13.7	42
3	Impact of processing conditions on the film formation of lead-free halide double perovskite Cs ₂ AgBiBr ₆ . Journal of Materials Chemistry A, 2022, 10, 19868-19880.	5.2	12
4	Spatiotemporal mapping of microscopic strains and defects to reveal Li-dendrite-induced failure in all-solid-state batteries. Materials Today, 2022, 57, 180-191.	8.3	12
5	Quantification of room temperature strengthening of laser shock peened Ni-based superalloy using synchrotron microdiffraction. Materials and Design, 2022, 221, 110948.	3.3	5
6	Crystal nucleation and growth of spherulites demonstrated by coral skeletons and phase-field simulations. Acta Biomaterialia, 2021, 120, 277-292.	4.1	21
7	On the Pressure Generated by Thermite Reactions Using Stressâ€Altered Aluminum Particles. Propellants, Explosives, Pyrotechnics, 2021, 46, 99-106.	1.0	6
8	Antiphase resonance at X-ray irradiated microregions in amorphous Fe80B20 stripes. Journal of Magnetism and Magnetic Materials, 2021, 520, 167017.	1.0	3
9	Influence of dislocations and twin walls in BaTiO3 on the voltage-controlled switching of perpendicular magnetization. Physical Review Materials, 2021, 5, .	0.9	3
10	Fleetite, Cu2RhIrSb2, a New Species of Platinum-Group Mineral from the Miass Placer Zone, Southern Urals, Russia. Canadian Mineralogist, 2021, 59, 423-430.	0.3	1
11	Twinning-mediated anomalous alignment of rutile films revealed by synchrotron X-ray nanodiffraction. IScience, 2021, 24, 102278.	1.9	1
12	Localized strain profile in surface electrode array for programmable composite multiferroic devices. Applied Physics Letters, 2021, 118, .	1.5	5
13	Energy Conversion from Heat to Electricity by Highly Reversible Phase-Transforming Ferroelectrics. Physical Review Applied, 2021, 16, .	1.5	4
14	Spin waves excitation at micron-sized, anisotropy modified regions in amorphous Fe80B20 stripes: Local properties and inter-regions coupling. Materials Science and Engineering B: Solid-State Materials for Advanced Technology, 2021, 271, 115258.	1.7	6
15	Out-of-equilibrium processes in crystallization of organic-inorganic perovskites during spin coating. Nature Communications, 2021, 12, 5624.	5.8	53
16	Pressure-induced suppression of Jahn–Teller distortions and enhanced electronic properties in high-entropy oxide (Mg0.2Ni0.2Co0.2Zn0.2Cu0.2)O. Applied Physics Letters, 2021, 119, .	1.5	4
17	Unnamed Pt(Cu0.67Sn0.33) from the Bolshoy Khailyk River, Western Sayans, Russia, and a Review of Related Compounds and Solid Solutions. Minerals (Basel, Switzerland), 2021, 11, 1240.	0.8	0
18	Ferrotorryweiserite, Rh5Fe10S16, a New Mineral Species from the Sisim Placer Zone, Eastern Sayans, Russia, and the Torryweiserite–Ferrotorryweiserite Series. Minerals (Basel, Switzerland), 2021, 11, 1420	0.8	2

#	Article	IF	CITATIONS
19	Scalable Freeze-Tape-Casting Fabrication and Pore Structure Analysis of 3D LLZO Solid-State Electrolytes. ACS Applied Materials & Interfaces, 2020, 12, 3494-3501.	4.0	52
20	In situ study of rotating lattice singleâ€crystal formation in Sb 2 S 3 glass by Laue μXRD. Journal of the American Ceramic Society, 2020, 103, 3954-3961.	1.9	1
21	Revealing the Dynamics of Hybrid Metal Halide Perovskite Formation via Multimodal In Situ Probes. Advanced Functional Materials, 2020, 30, 1908337.	7.8	40
22	In-situ, microscale characterization of heterogeneous deformation around notch in martensitic Shape Memory Alloy. Materials Science & Engineering A: Structural Materials: Properties, Microstructure and Processing, 2020, 771, 138605.	2.6	1
23	<i>XtalCAMP</i> : a comprehensive program for the analysis and visualization of scanning Laue X-ray micro-/nanodiffraction data. Journal of Applied Crystallography, 2020, 53, 1392-1403.	1.9	7
24	Two-Tier Compatibility of Superelastic Bicrystal Micropillar at Grain Boundary. Nano Letters, 2020, 20, 8332-8338.	4.5	8
25	Derived crystal structure of martensitic materials by solid–solid phase transformation. Acta Crystallographica Section A: Foundations and Advances, 2020, 76, 521-533.	0.0	3
26	Residual lattice strain in quartzites as a potential palaeo-piezometer. Geophysical Journal International, 2020, 222, 1363-1378.	1.0	7
27	Synthesis and characterization of Pt(Cu0.67Sn0.33). Solid State Sciences, 2020, 105, 106282.	1.5	1
28	Potential Control of Oxygen Non-Stoichiometry in Cerium Oxide and Phase Transition Away from Equilibrium. ACS Applied Materials & amp; Interfaces, 2020, 12, 31514-31521.	4.0	12
29	Mapping of Heterogeneous Catalyst Degradation in Polymer Electrolyte Fuel Cells. Advanced Energy Materials, 2020, 10, 2000623.	10.2	24
30	X-ray Laue Microdiffraction and Raman Spectroscopic Investigation of Natural Silicon and Moissanite. Minerals (Basel, Switzerland), 2020, 10, 204.	0.8	2
31	Highly Enhanced Curie Temperature in Gaâ€Implanted Fe ₃ GeTe ₂ van der Waals Material. Advanced Quantum Technologies, 2020, 3, 2000017.	1.8	34
32	Raftingâ€Enabled Recovery Avoids Recrystallization in 3Dâ€Printingâ€Repaired Singleâ€Crystal Superalloys. Advanced Materials, 2020, 32, e1907164.	11.1	28
33	High-pressure strengthening in ultrafine-grained metals. Nature, 2020, 579, 67-72.	13.7	96
34	Multi-scale microstructural investigation of a laser 3D printed Ni-based superalloy. Additive Manufacturing, 2020, 34, 101220.	1.7	12
35	Black carbon enriches short-range-order ferrihydrite in Amazonian Dark Earth: Interplay mechanism and environmental implications. Science of the Total Environment, 2020, 725, 138195.	3.9	6
36	Resistive contribution in electrical-switching experiments with antiferromagnets. Physical Review Research, 2020, 2, .	1.3	25

#	Article	IF	CITATIONS
37	Pattern-matching indexing of Laue and monochromatic serial crystallography data for applications in materials science. Journal of Applied Crystallography, 2020, 53, 824-836.	1.9	5
38	Oriented porous LLZO 3D structures obtained by freeze casting for battery applications. Journal of Materials Chemistry A, 2019, 7, 20861-20870.	5.2	65
39	Authigenic Mineral Texture in Submarine 1979 Basalt Drill Core, Surtsey Volcano, Iceland. Geochemistry, Geophysics, Geosystems, 2019, 20, 3751-3773.	1.0	10
40	Volcanoes Erupt Stressed Quartz Crystals. Geophysical Research Letters, 2019, 46, 8791-8800.	1.5	2
41	Stability and Compressibility of Cation-Doped High-Entropy Oxide MgCoNiCuZnO ₅ . Journal of Physical Chemistry C, 2019, 123, 17735-17744.	1.5	50
42	Stress and Fracture of Crystalline Silicon Cells in Solar Photovoltaic Modules – A Synchrotron X-ray Microdiffraction based Investigation. MRS Advances, 2019, 4, 2319-2335.	0.5	5
43	Lattice strain causes non-radiative losses in halide perovskites. Energy and Environmental Science, 2019, 12, 596-606.	15.6	343
44	Thermomechanical residual stress evaluation in multi-crystalline silicon solar cells of photovoltaic modules with different encapsulation polymers using synchrotron X-ray microdiffraction. Solar Energy Materials and Solar Cells, 2019, 193, 387-402.	3.0	21
45	Slags as Evidence for Copper Mining above Casaccia, Val Bregaglia (Central Alps). Minerals (Basel,) Tj ETQq1 1 (0.784314 r 0.8	gBŢ_/Overlo <mark>ck</mark>
46	Helical van der Waals crystals with discretized Eshelby twist. Nature, 2019, 570, 358-362.	13.7	91
47	Platiniferous Tetra-Auricupride: A Case Study from the Bolshoy Khailyk Placer Deposit, Western Sayans, Russia. Minerals (Basel, Switzerland), 2019, 9, 160.	0.8	5
48	Stress evolution in silicon nanowires during electrochemical lithiation using in situ synchrotron X-ray microdiffraction. Journal of Materials Research, 2019, 34, 1622-1631.	1.2	10
49	Stress Relaxation Related to Spontaneous Thin Film Buckling: Correlation between Finite Element Calculations and Micro Diffraction Analysis. Quantum Beam Science, 2019, 3, 1.	0.6	4
50	Fallout melt debris and aerodynamically-shaped glasses in beach sands of Hiroshima Bay, Japan. Anthropocene, 2019, 25, 100196.	1.6	8
51	Thermal stability of laser shock peening processed Ni-based superalloy DZ17G. IOP Conference Series: Materials Science and Engineering, 2019, 580, 012059.	0.3	0
52	Data-driven approach for synchrotron X-ray Laue microdiffraction scan analysis. Acta Crystallographica Section A: Foundations and Advances, 2019, 75, 876-888.	0.0	10
53	Light-driven anaerobic microbial oxidation of manganese. Nature, 2019, 576, 311-314.	13.7	90
54	Highly reactive energetic films by pre-stressing nano-aluminum particles. RSC Advances, 2019, 9, 40607-40617.	1.7	5

#	Article	IF	CITATIONS
55	Probing the <i>in situ</i> dynamics of structure–property evolution in hybrid perovskite thin films spincoated from complex fluids by a custom-designed beamline-compatible multimodal measurement chamber. Acta Crystallographica Section A: Foundations and Advances, 2019, 75, a155-a156.	0.0	6
56	Influence of Nonuniform Micron-Scale Strain Distributions on the Electrical Reorientation of Magnetic Microstructures in a Composite Multiferroic Heterostructure. Nano Letters, 2018, 18, 1952-1961.	4.5	44
57	Mechanism of heat affected zone cracking in Ni-based superalloy DZ125L fabricated by laser 3D printing technique. Materials and Design, 2018, 150, 171-181.	3.3	57
58	A study of deformation and strain induced in bulk by the oxide layers formation on a Fe-Cr-Al alloy in high-temperature liquid Pb-Bi eutectic. Acta Materialia, 2018, 151, 301-309.	3.8	25
59	Cation-Dependent Light-Induced Halide Demixing in Hybrid Organic–Inorganic Perovskites. Nano Letters, 2018, 18, 3473-3480.	4.5	65
60	A peak position comparison method for high-speed quantitative Laue microdiffraction data processing. Scripta Materialia, 2018, 143, 49-53.	2.6	18
61	Fabrication of single crystal architecture in Sb-S-I glass: Transition from dot to line. Journal of Non-Crystalline Solids, 2018, 501, 43-48.	1.5	4
62	Ferroelastic domain structure and phase transition in single-crystalline [PbZn1/3Nb2/3O3]1-x[PbTiO3]x observed via in situ x-ray microbeam. Journal of the European Ceramic Society, 2018, 38, 1488-1497.	2.8	4
63	Probing Plasticity and Strain-Rate Effects of Indium Submicron Pillars Using Synchrotron Laue X-Ray Microdiffraction. IEEE Transactions on Device and Materials Reliability, 2018, 18, 490-497.	1.5	6
64	X-ray diffraction and heterogeneous materials: An adaptive crystallography approach. Comptes Rendus Physique, 2018, 19, 553-560.	0.3	3
65	Molecular Weaving of Covalent Organic Frameworks for Adaptive Guest Inclusion. Journal of the American Chemical Society, 2018, 140, 16015-16019.	6.6	107
66	Impact ignition and combustion of micron-scale aluminum particles pre-stressed with different quenching rates. Journal of Applied Physics, 2018, 124, .	1.1	14
67	New Structural Insight into Interface-Controlled α–σ Phase Transformation in Fe-Cr Alloys. Quantum Beam Science, 2018, 2, 27.	0.6	2
68	Synchrotron X-ray Microdiffraction and Fluorescence Imaging of Mineral and Rock Samples. Journal of Visualized Experiments, 2018, , .	0.2	3
69	Probing Stress States in Silicon Nanowires During Electrochemical Lithiation Using In Situ Synchrotron X-Ray Microdiffraction. Frontiers in Energy Research, 2018, 6, .	1.2	17
70	Quantitative Scanning Laue Diffraction Microscopy: Application to the Study of 3D Printed Nickel-Based Superalloys. Quantum Beam Science, 2018, 2, 13.	0.6	12
71	xmlns:mml="http://www.w3.org/1998/Math/MathML" display="inline"> <mml:mrow><mml:msub><mml:mrow><mml:mi>BaFe</mml:mi></mml:mrow><mml:mrow>< stretchy="false">(<mml:mi>As</mml:mi><mml:mo>,</mml:mo><mml:mi) 0.784314="" 1="" etqq1="" rg<="" td="" tj=""><td>mml;mn>2 BT /Overloc</td><td><!--<br-->k 10 ff 50 92</td></mml:mi)></mml:mrow></mml:msub></mml:mrow>	mml;mn>2 BT /Overloc	<br k 10 ff 50 92
72	X-Ray Diffraction under Extreme Conditions at the Advanced Light Source. Quantum Beam Science,	0.6	18

72 2018, 2, 4.

#	Article	IF	CITATIONS
73	Reversal in the Size Dependence of Grain Rotation. Physical Review Letters, 2017, 118, 096101.	2.9	26
74	Probing stress and fracture mechanism in encapsulated thin silicon solar cells by synchrotron X-ray microdiffraction. Solar Energy Materials and Solar Cells, 2017, 162, 30-40.	3.0	39
75	From cells to laminate: probing and modeling residual stress evolution in thin silicon photovoltaic modules using synchrotron Xâ€ray microâ€diffraction experiments and finite element simulations. Progress in Photovoltaics: Research and Applications, 2017, 25, 791-809.	4.4	47
76	Statistical study of ductility-dip cracking induced plastic deformation in polycrystalline laser 3D printed Ni-based superalloy. Scientific Reports, 2017, 7, 2859.	1.6	19
77	In-situ studies on martensitic transformation and high-temperature shape memory in small volume zirconia. Acta Materialia, 2017, 134, 257-266.	3.8	26
78	Measuring grain rotation at the nanoscale. High Pressure Research, 2017, 37, 287-295.	0.4	2
79	Laser Fabrication of Two-Dimensional Rotating-Lattice Single Crystal. Crystal Growth and Design, 2017, 17, 1735-1746.	1.4	14
80	Nacre tablet thickness records formation temperature in modern and fossil shells. Earth and Planetary Science Letters, 2017, 460, 281-292.	1.8	51
81	Synchrotron X-ray Analytical Techniques for Studying Materials Electrochemistry in Rechargeable Batteries. Chemical Reviews, 2017, 117, 13123-13186.	23.0	390
82	Parrotfish Teeth: Stiff Biominerals Whose Microstructure Makes Them Tough and Abrasion-Resistant To Bite Stony Corals. ACS Nano, 2017, 11, 11856-11865.	7.3	37
83	Amorphous calcium carbonate particles form coral skeletons. Proceedings of the National Academy of Sciences of the United States of America, 2017, 114, E7670-E7678.	3.3	243
84	Synthesis of monodisperse CeO ₂ –ZrO ₂ particles exhibiting cyclic superelasticity over hundreds of cycles. Journal of the American Ceramic Society, 2017, 100, 4199-4208.	1.9	15
85	Residual stress determination in oxide layers at different length scales combining Raman spectroscopy and X-ray diffraction: Application to chromia-forming metallic alloys. Journal of Applied Physics, 2017, 122, .	1.1	13
86	Elemental Topological Dirac Semimetal: <mml:math xmlns:mml="http://www.w3.org/1998/Math/MathML" display="inline"><mml:mi>α</mml:mi> -Sn on InSb(111). Physical Review Letters, 2017, 118, 146402.</mml:math 	2.9	98
87	Probing Plasticity Mechanisms in Low Melting Temperature Metallic Nanostructures Using Synchrotron X-Ray Microdiffraction. Procedia Engineering, 2017, 215, 246-262.	1.2	4
88	Enabling the study of stress states using in situ µSXRD in the silicon nanowire anode during electrochemical lithiation in a specially designed Li-ion battery test cell. Procedia Engineering, 2017, 215, 263-275.	1.2	7
89	<i>In-situ</i> characterization of highly reversible phase transformation by synchrotron X-ray Laue microdiffraction. Applied Physics Letters, 2016, 108, .	1.5	13
90	Synthesizing skyrmion bound pairs in Fe-Gd thin films. Applied Physics Letters, 2016, 109, .	1.5	67

#	Article	IF	CITATIONS
91	Effect of interconnect plasticity on soldering induced residual stress in thin crystalline silicon solar cells. , 2016, , .		6
92	Understanding size effects in the advanced through-silicon via interconnect schemes for 3D ICs. , 2016, , .		1
93	MultiLaue: A Technique to Extract d-spacings from Laue XRD. Microscopy and Microanalysis, 2016, 22, 1784-1785.	0.2	1
94	Hardness and microstructural inhomogeneity at the epitaxial interface of laser 3D-printed Ni-based superalloy. Applied Physics Letters, 2016, 109, .	1.5	13
95	In situ synchrotron study of electromigration induced grain rotations in Sn solder joints. Scientific Reports, 2016, 6, 24418.	1.6	16
96	Real-time data-intensive computing. AIP Conference Proceedings, 2016, , .	0.3	10
97	Phase transformation and fluorescent enhancement of ErF3 at high pressure. Solid State Communications, 2016, 242, 30-35.	0.9	6
98	Determination of the stretch tensor for structural transformations. Journal of the Mechanics and Physics of Solids, 2016, 93, 34-43.	2.3	41
99	A slice of an aluminum particle: Examining grains, strain and reactivity. Combustion and Flame, 2016, 173, 229-234.	2.8	10
100	Probing Phase Transformations and Microstructural Evolutions at the Small Scales: Synchrotron X-ray Microdiffraction for Advanced Applications in 3D IC (Integrated Circuits) and Solar PV (Photovoltaic) Devices. Journal of Electronic Materials, 2016, 45, 6222-6232.	1.0	42
101	Real-time microstructure imaging by Laue microdiffraction: A sample application in laser 3D printed Ni-based superalloys. Scientific Reports, 2016, 6, 28144.	1.6	18
102	Effect of scaling copper through-silicon vias on stress and reliability for 3D interconnects. , 2016, , .		9
103	Rotating lattice single crystal architecture on the surface of glass. Scientific Reports, 2016, 6, 36449.	1.6	22
104	Quantitative microstructural imaging by scanning Laue x-ray micro- and nanodiffraction. MRS Bulletin, 2016, 41, 445-453.	1.7	38
105	Stress relaxation in pre-stressed aluminum core–shell particles: X-ray diffraction study, modeling, and improved reactivity. Combustion and Flame, 2016, 170, 30-36.	2.8	12
106	Critical Temperature Shift for Stress Induced Voiding in Advanced Cu Interconnects for 32 nm and Beyond. Procedia Engineering, 2016, 139, 32-40.	1.2	1
107	Synchrotron X-ray Micro-diffraction – Probing Stress State in Encapsulated Thin Silicon Solar Cells. Procedia Engineering, 2016, 139, 123-133.	1.2	31
108	On the Mechanical Stresses of Cu Through-Silicon Via (TSV) Samples Fabricated by SK Hynix vs. SEMATECH – Enabling Robust and Reliable 3-D Interconnect/Integrated Circuit (IC) Technology. Procedia Engineering, 2016, 139, 101-111.	1.2	40

#	Article	IF	CITATIONS
109	Microstructure, crystallization and shape memory behavior of titania and yttria co-doped zirconia. Journal of the European Ceramic Society, 2016, 36, 1277-1283.	2.8	35
110	Improving aluminum particle reactivity by annealing and quenching treatments: Synchrotron X-ray diffraction analysis of strain. Acta Materialia, 2016, 103, 495-501.	3.8	19
111	Experimental Stress Characterization and Numerical Simulation for Copper Pumping Analysis of Through-Silicon Vias. IEEE Transactions on Components, Packaging and Manufacturing Technology, 2016, 6, 993-999.	1.4	4
112	Low Stress Encapsulants? Influence of Encapsulation Materials on Stress and Fracture of Thin Silicon Solar Cells as Revealed by Synchrotron X-ray Submicron Diffraction. Procedia Engineering, 2016, 139, 76-86.	1.2	17
113	Controlling the Temperature and Speed of the Phase Transition of VO ₂ Microcrystals. ACS Applied Materials & Interfaces, 2016, 8, 2280-2286.	4.0	44
114	Impact of deposition conditions on the crystallization kinetics of amorphous GeTe films. Journal of Materials Science, 2016, 51, 1864-1872.	1.7	34
115	Effect of Au/Pd surface finishing on metastable Sn phase formation in microbumps. , 2015, , .		0
116	A synchrotron study of microstructure gradient in laser additively formed epitaxial Ni-based superalloy. Scientific Reports, 2015, 5, 14903.	1.6	21
117	Ferroelectric soft mode of polarZnTiO3investigated by Raman spectroscopy at high pressure. Physical Review B, 2015, 91, .	1.1	15
118	A synchrotron study of defect and strain inhomogeneity in laser-assisted three-dimensionally-printed Ni-based superalloy. Applied Physics Letters, 2015, 107, .	1.5	31
119	Complementary use of monochromatic and white-beam X-ray micro-diffraction for the investigation of ancient materials. Journal of Applied Crystallography, 2015, 48, 1522-1533.	1.9	18
120	Evolution of terra sigillata technology from Italy to Gaul through a multi-technique approach. Journal of Analytical Atomic Spectrometry, 2015, 30, 658-665.	1.6	20
121	Effect of Surface Microstructure on Electrochemical Performance of Garnet Solid Electrolytes. ACS Applied Materials & Interfaces, 2015, 7, 2073-2081.	4.0	347
122	Deformation patterns in cross-sections of twisted bamboo-structured Au microwires. Acta Materialia, 2015, 97, 216-222.	3.8	25
123	Plasticity evolution in nanoscale Cu/Nb single-crystal multilayers as revealed by synchrotron X-ray microdiffraction. Materials Science & Engineering A: Structural Materials: Properties, Microstructure and Processing, 2015, 635, 6-12.	2.6	56
124	A metastable phase of tin in 3D integrated circuit solder microbumps. Scripta Materialia, 2015, 102, 39-42.	2.6	18
125	Residual stress preserved in quartz from the San Andreas Fault Observatory at Depth. Geology, 2015, 43, 219-222.	2.0	33
126	Mobile metallic domain walls in an all-in-all-out magnetic insulator. Science, 2015, 350, 538-541.	6.0	159

#	Article	IF	CITATIONS
127	Internal stresses in pre-stressed micron-scale aluminum core-shell particles and their improved reactivity. Journal of Applied Physics, 2015, 118, .	1.1	9
128	Microscopic Cracking on Flat Alloy 600 Surfaces Following Accelerated Caustic Corrosion: Mapping of Strains and Microstructure During the Corrosion Process. Corrosion, 2015, 71, 65-70.	0.5	2
129	Serial snapshot crystallography for materials science with SwissFEL. IUCrJ, 2015, 2, 361-370.	1.0	19
130	A concise synchrotron X-ray microdiffraction field guide for the Earth scientists. Boletin De La Sociedad Geologica Mexicana, 2015, 67, 467-478.	0.1	1
131	High performance data management and analysis for tomography. Proceedings of SPIE, 2014, , .	0.8	11
132	Relationship between Residual Stresses and Damaging in Thermally Grown Oxide on Metals: Raman Spectroscopy and Synchrotron Micro-Diffraction Contributions. Advances in Science and Technology, 2014, 91, 100-107.	0.2	0
133	Time and spatial resolution of slip and twinning in a grain embedded within a magnesium polycrystal. Acta Materialia, 2014, 78, 203-212.	3.8	33
134	<i>In-situ</i> microscale through-silicon via strain measurements by synchrotron x-ray microdiffraction exploring the physics behind data interpretation. Applied Physics Letters, 2014, 105, .	1.5	21
135	Study of Stresses and Plasticity in Through-Silicon Via Structures for 3D Interconnects by X-Ray Micro-Beam Diffraction. IEEE Transactions on Device and Materials Reliability, 2014, 14, 698-703.	1.5	15
136	Crystal Structure of an Indigo@Silicalite Hybrid Related to the Ancient Maya Blue Pigment. Journal of Physical Chemistry C, 2014, 118, 28032-28042.	1.5	26
137	XMAS: A Versatile Tool for Analyzing Synchrotron X-ray Microdiffraction Data. , 2014, , 125-155.		65
138	Mapping of Microscopic Strain Distributions in an Alloy 600 C-Ring After Application of Hoop Stresses and Stress Corrosion Cracking. Corrosion, 2014, 70, 66-73.	0.5	5
139	Enabling thin silicon technologies for next generation c-Si solar PV renewable energy systems using synchrotron X-ray microdiffraction as stress and crack mechanism probe. Solar Energy Materials and Solar Cells, 2014, 130, 303-308.	3.0	54
140	Learning from the past: Rare ε-Fe2O3 in the ancient black-glazed Jian (Tenmoku) wares. Scientific Reports, 2014, 4, 4941.	1.6	100
141	Acquisition, Sharing, and Processing of Large Data Sets for Strain Imaging: An Example of an Indented Ni3Al/Mo Composite. Jom, 2013, 65, 29-34.	0.9	2
142	Crystal nucleation and near-epitaxial growth in nacre. Journal of Structural Biology, 2013, 184, 454-463.	1.3	54
143	Metal insulator transition characteristics of macro-size single domain VO ₂ crystals. Phase Transitions, 2013, 86, 941-946.	0.6	4
144	Crystal lattice tilting in prismatic calcite. Journal of Structural Biology, 2013, 183, 180-190.	1.3	63

#	Article	IF	CITATIONS
145	Influence of bulk pre-straining on the size effect in nickel compression pillars. Materials Science & Engineering A: Structural Materials: Properties, Microstructure and Processing, 2013, 559, 147-158.	2.6	59
146	Methodology for optimalin situalignment and setting of bendable optics for nearly diffraction-limited focusing of soft x-rays. Optical Engineering, 2013, 52, 033603.	0.5	17
147	Using a non-monochromatic microbeam for serial snapshot crystallography. Journal of Applied Crystallography, 2013, 46, 791-794.	1.9	27
148	Thermomechanical strain measurements by synchrotron x-ray diffraction and data interpretation for through-silicon vias. Applied Physics Letters, 2013, 103, .	1.5	19
149	Plasticity mechanism for copper extrusion in through-silicon vias for three-dimensional interconnects. Applied Physics Letters, 2013, 103, .	1.5	57
150	Can Laue microdiffraction be used to solve and refine complex inorganic structures?. Journal of Applied Crystallography, 2013, 46, 1805-1816.	1.9	17
151	Role of joule heating effect and bulk-surface phases in voltage-driven metal-insulator transition in VO2 crystal. Applied Physics Letters, 2013, 103, .	1.5	59
152	Dimension and liner dependent thermomechanical strain characterization of through-silicon vias using synchrotron x-ray diffraction. Journal of Applied Physics, 2013, 114, 064908.	1.1	16
153	X-Ray Microdiffraction of Biominerals. Methods in Enzymology, 2013, 532, 501-531.	0.4	15
154	Bendable Kirkpatrick-Baez mirrors for the ALS micro-diffraction beamline 12.3.2: optimal tuning and alignment for multiple focusing geometries. Journal of Physics: Conference Series, 2013, 425, 152004.	0.3	3
155	Experimental methods for optimal tuning of bendable mirrors for diffraction-limited soft x-ray focusing. Journal of Physics: Conference Series, 2013, 425, 152003.	0.3	6
156	Studies of microscopic strains on Alloy 600 surfaces arising from stress corrosion cracking. , 2013, , .		0
157	Using a non-monochromatic microbeam for serial snapshot crystallography. Acta Crystallographica Section A: Foundations and Advances, 2013, 69, s26-s26.	0.3	0
158	Critical temperature shift for Stress Induced Voiding in advanced Cu interconnects for 32 nm and beyond. , 2012, , .		5
159	Directed assembly of nano-scale phase variants in highly strained BiFeO3 thin films. Journal of Applied Physics, 2012, 112, 064102.	1.1	35
160	Comparison of mechanical stresses of Cu Through-Silicon Via (TSV) samples fabricated by Hynix vs. SEMATECH using synchrotron X-ray microdiffraction for 3-D integration and reliability. , 2012, , .		6
161	Preferred orientation of 30 μm fine pitch Sn2.5Ag micro-bumps studied by synchrotron polychromatic x-ray Laue microdiffraction. , 2012, , .		1
162	High-Performance Parallel and Stream Processing of X-ray Microdiffraction Data on Multicores. Journal of Physics: Conference Series, 2012, 341, 012025.	0.3	1

#	Article	IF	CITATIONS
163	Methodology for optimal in situ alignment and setting of bendable optics for diffraction-limited focusing of soft x-rays. , 2012, , .		4
164	Plasticity in the nanoscale Cu/Nb single-crystal multilayers as revealed by synchrotron Laue x-ray microdiffraction. Journal of Materials Research, 2012, 27, 599-611.	1.2	49
165	Experimental and numerical study of the effects of a nanocrystallisation treatment on high-temperature oxidation of a zirconium alloy. Corrosion Science, 2012, 60, 224-230.	3.0	13
166	Plastic and elastic strains in short and long cracks in Alloy 600 studied by polychromatic X-ray microdiffraction and electron backscatter diffraction. Acta Materialia, 2012, 60, 5508-5515.	3.8	7
167	Microstructure Evolution and Defect Formation in Cu Through-Silicon Vias (TSVs) During Thermal Annealing. Journal of Electronic Materials, 2012, 41, 712-719.	1.0	67
168	The study of stress application and corrosion cracking on Ni–16 Cr–9 Fe (Alloy 600) C-ring samples by polychromatic X-ray microdiffraction. Acta Materialia, 2012, 60, 781-792.	3.8	13
169	Measurement of stresses in Cu and Si around through-silicon via by synchrotron X-ray microdiffraction for 3-dimensional integrated circuits. Microelectronics Reliability, 2012, 52, 530-533.	0.9	133
170	Plasticity of indium nanostructures as revealed by synchrotron X-ray microdiffraction. Materials Science & Engineering A: Structural Materials: Properties, Microstructure and Processing, 2012, 538, 89-97.	2.6	31
171	Biomineral nanoparticles are space-filling. Nanoscale, 2011, 3, 603-609.	2.8	64
172	Evidence for high stress in quartz from the impact site of Vredefort, South Africa. European Journal of Mineralogy, 2011, 23, 169-178.	0.4	19
173	Preferred orientation relationships with large misfit interfaces between Ni3Sn4 and Ni in reactive wetting of eutectic SnPb on Ni. Journal of Applied Physics, 2011, 109, 123513.	1.1	8
174	Fate of arsenic-bearing phases during the suspended transport in a gold mining district (Isle river) Tj ETQq0 0 0 $r_{ m s}$	gB <u>T</u> /Overl	ock_10 Tf 50
175	Observation of insulating–insulating monoclinic structural transition in macroâ€ s ized VO ₂ single crystals. Physica Status Solidi - Rapid Research Letters, 2011, 5, 107-109.	1.2	23
176	Deformation twinning and residual stress in calcite studied with synchrotron polychromatic X-ray microdiffraction. Physics and Chemistry of Minerals, 2011, 38, 491-500.	0.3	18
177	Fabrication, microstructure, and mechanical properties of tin nanostructures. Materials Science & Engineering A: Structural Materials: Properties, Microstructure and Processing, 2011, 528, 5822-5832.	2.6	54
178	Determining the energy-dependent X-ray flux variation of a synchrotron beamline using Laue diffraction patterns. Journal of Applied Crystallography, 2011, 44, 177-183.	1.9	10
179	Structure and Mechanical Properties of a Pteropod Shell Consisting of Interlocked Helical Aragonite Nanofibers. Angewandte Chemie - International Edition, 2011, 50, 10361-10365.	7.2	43
180	Grain boundary effects on the mechanical properties of bismuth nanostructures. Acta Materialia, 2011, 59, 4709-4718.	3.8	30

#	Article	IF	CITATIONS
181	Growth and structural characterization of epitaxial Cu/Nb multilayers. Thin Solid Films, 2011, 519, 4137-4143.	0.8	45
182	Nonpercolative metal-insulator transition in VO <mml:math xmlns:mml="http://www.w3.org/1998/Math/MathML" display="inline"><mml:msub><mml:mrow /><mml:mn>2</mml:mn></mml:mrow </mml:msub>single crystals. Physical Review B, 2011, 84, .</mml:math 	1.1	39
183	The Study of Stress Corrosion Cracking on Alloy 600 C-Ring Samples by Polychromatic X-Ray Microdiffraction. , 2011, , 1773-1785.		0
184	Investigation of cyclic impact fatigue, grain-to-grain interaction, and residual stress in zirconia dental materials. Conference Proceedings of the Society for Experimental Mechanics, 2011, , 399-406.	0.3	0
185	The nature of marbled Terra Sigillata slips: a combined μXRF andÂμXRD investigation. Applied Physics A: Materials Science and Processing, 2010, 99, 419-425.	1.1	24
186	Fabrication, structure and mechanical properties of indium nanopillars. Acta Materialia, 2010, 58, 1361-1368.	3.8	36
187	Evolution of ferroelectric domain structures embedded inside polycrystalline BaTiO3 during heating. Journal of Applied Physics, 2010, 107, .	1.1	5
188	High precision thermal stress study on flip chips by synchrotron polychromatic x-ray microdiffraction. Journal of Applied Physics, 2010, 107, 063502.	1.1	14
189	ALS Users Meeting and Workshops. Synchrotron Radiation News, 2010, 23, 2-14.	0.2	0
190	Visualization of Charge Distribution in a Lithium Battery Electrode. Journal of Physical Chemistry Letters, 2010, 1, 2120-2123.	2.1	155
191	Extended Mapping and Exploration of the Vanadium Dioxide Stress-Temperature Phase Diagram. Nano Letters, 2010, 10, 2667-2673.	4.5	215
192	Sulfide oxidation observed using micro-Raman spectroscopy and micro-X-ray diffraction: The importance of water/rock ratios and pH conditions. American Mineralogist, 2010, 95, 582-591.	0.9	29
193	Constant threshold resistivity in the metal-insulator transition of <mml:math xmlns:mml="http://www.w3.org/1998/Math/MathML" display="inline"> <mml:mrow> <mml:msub> <mml:mrow> <mml:mtext>VO </mml:mtext> </mml:mrow> <mml:mn>. Physical Review B, 2010, 82.</mml:mn></mml:msub></mml:mrow></mml:math 	2< 11 11 mml:m	n> ⁴ 2/mml:msi
194	Synchrotron X-Ray Microdiffraction Studies of Electromigration in Interconnect lines at the Advanced Light Source. , 2009, , .		1
195	A dedicated superbend x-ray microdiffraction beamline for materials, geo-, and environmental sciences at the advanced light source. Review of Scientific Instruments, 2009, 80, 035108.	0.6	161
196	In situmeasurement of electromigration-induced transient stress in Pb-free Sn–Cu solder joints by synchrotron radiation based x-ray polychromatic microdiffraction. Journal of Applied Physics, 2009, 106, 023502.	1.1	26
197	Ultrafast growth of wadsleyite in shock-produced melts and its implications for early solar system impact processes. Proceedings of the National Academy of Sciences of the United States of America, 2009, 106, 13691-13695.	3.3	36
198	Evidence for residual elastic strain in deformed natural quartz. American Mineralogist, 2009, 94, 1059-1062.	0.9	24

#	Article	IF	CITATIONS
199	Mapping mesoscale heterogeneity in the plastic deformation of a copper single crystal. Philosophical Magazine, 2009, 89, 77-107.	0.7	30
200	Electromigration-Induced Plasticity: Texture Correlation and Implications for Reliability Assessment. Journal of Electronic Materials, 2009, 38, 379-391.	1.0	35
201	Preferred orientation of ettringite in concrete fractures. Journal of Applied Crystallography, 2009, 42, 429-432.	1.9	13
202	A superbend X-ray microdiffraction beamline at the advanced light source. Materials Science & Engineering A: Structural Materials: Properties, Microstructure and Processing, 2009, 524, 28-32.	2.6	56
203	Mechanism of Calcite Co-Orientation in the Sea Urchin Tooth. Journal of the American Chemical Society, 2009, 131, 18404-18409.	6.6	181
204	Spatially Resolved U(VI) Partitioning and Speciation: Implications for Plume Scale Behavior of Contaminant U in the Hanford Vadose Zone. Environmental Science & Technology, 2009, 43, 2247-2253.	4.6	8
205	A search for evidence of strain gradient hardening in Au submicron pillars under uniaxial compression using synchrotron X-ray microdiffraction. Acta Materialia, 2008, 56, 602-608.	3.8	90
206	The passivation of calcite by acid mine water. Column experiments with ferric sulfate and ferric chloride solutions at pH 2. Applied Geochemistry, 2008, 23, 3579-3588.	1.4	37
207	Oxidation kinetics of high strength low alloy steels at elevated temperatures. Corrosion Science, 2008, 50, 2804-2815.	3.0	24
208	Gradual Ordering in Red Abalone Nacre. Journal of the American Chemical Society, 2008, 130, 17519-17527.	6.6	126
209	In-situ early stage electromigration study in Al line using synchrotron polychromatic X-ray microdiffraction. Materials Research Society Symposia Proceedings, 2008, 1079, 1.	0.1	1
210	Plastic deformation in Al (Cu) interconnects stressed by electromigration and studied by synchrotron polychromatic x-ray microdiffraction. Journal of Applied Physics, 2008, 104, .	1.1	43
211	In-situ Study of Electromigration-induced Grain Rotation in Pb-free Solder Joint by Synchrotron Microdiffraction. Materials Research Society Symposia Proceedings, 2008, 1116, 506.	0.1	2
212	Indentation size effects in single crystal copper as revealed by synchrotron x-ray microdiffraction. Journal of Applied Physics, 2008, 104, 043501.	1.1	52
213	Electromigration-induced Plasticity and Texture in Cu Interconnects. AIP Conference Proceedings, 2007, , .	0.3	3
214	In-Situ White Beam Microdiffraction Study of the Deformation Behavior in Polycrystalline Magnesium Alloy During Uniaxial Loading. AlP Conference Proceedings, 2007, , .	0.3	1
215	Two-dimensional mapping of triaxial strain fields in a multiferroic BiFeO3 thin film using scanning x-ray microdiffraction. Applied Physics Letters, 2007, 90, 102904.	1.5	4
216	Plasticity-Amplified Diffusivity: Dislocation Cores as Fast Diffusion Paths in CU Interconnects. , 2007, ,		5

#	Article	IF	CITATIONS
217	A laboratory based system for Laue micro x-ray diffraction. Review of Scientific Instruments, 2007, 78, 023904.	0.6	14
218	Dramatic morphological change of scallop-type Cu6Sn5 formed on (001) single crystal copper in reaction between molten SnPb solder and Cu. Applied Physics Letters, 2007, 91, .	1.5	99
219	Influence of Taoism on the invention of the purple pigment used on the Qin terracotta warriors. Journal of Archaeological Science, 2007, 34, 1878-1883.	1.2	41
220	Spectroscopic Evidence for Uranium Bearing Precipitates in Vadose Zone Sediments at the Hanford 300-Area Site. Environmental Science & amp; Technology, 2007, 41, 4633-4639.	4.6	84
221	Application of white-beam X-ray microdiffraction for the study of mineralogical phase identification in ancient Egyptian pigments. Journal of Applied Crystallography, 2007, 40, 1089-1096.	1.9	13
222	Preferred orientation relationship between Cu6Sn5 scallop-type grains and Cu substrate in reactions between molten Sn-based solders and Cu. Journal of Applied Physics, 2007, 102, .	1.1	67
223	Residual stress analysis in micro- and nano-structured materials by X-ray diffraction. International Journal of Materials and Product Technology, 2006, 26, 354.	0.1	8
224	Meeting Report: Frontiers of Synchrotron-Based X-ray Microdiffraction. Synchrotron Radiation News, 2006, 19, 7-8.	0.2	0
225	Micro scanning X-ray diffraction study of Gallo-Roman Terra Sigillata ceramics. Applied Physics A: Materials Science and Processing, 2006, 83, 219-224.	1.1	35
226	A synchrotron radiation x-ray microdiffraction study on orientation relationships between a Cu6 Sn5 and Cu substrate in solder joints. Jom, 2006, 58, 63-66.	0.9	14
227	A Comparison of X-Ray Microdiffraction and Coherent Gradient Sensing in Measuring Discontinuous Curvatures in Thin Film: Substrate Systems. Journal of Applied Mechanics, Transactions ASME, 2006, 73, 723-729.	1.1	18
228	X-Ray Microdiffraction as a Probe to Reveal Flux Divergences in Interconnects. AIP Conference Proceedings, 2006, , .	0.3	5
229	Strains, Stresses and Elastic Properties in Polycrystalline Metallic Thin Films: In Situ Deformation Combined with X-Ray Diffraction and Simulation Experiments. Materials Science Forum, 2006, 524-525, 735-740.	0.3	2
230	White Beam Microdiffraction Experiments for the Determination of the Local Plastic Behaviour of Polycrystals. Materials Science Forum, 2006, 524-525, 103-108.	0.3	3
231	Electromigration-Induced Plastic Deformation in Cu Damascene Interconnect Lines as Revealed by Synchrotron X-Ray Microdiffraction. Materials Research Society Symposia Proceedings, 2006, 914, 1.	0.1	11
232	Crystal plasticity in Cu damascene interconnect lines undergoing electromigration as revealed by synchrotron x-ray microdiffraction. Applied Physics Letters, 2006, 88, 233515.	1.5	100
233	D075 4-D XRD for strain in many grains using triangulation. Powder Diffraction, 2006, 21, 184-184.	0.4	3
234	Mechanism and Prevention of Spontaneous Tin Whisker Growth. Materials Transactions, 2005, 46, 2300-2308.	0.4	36

#	Article	IF	CITATIONS
235	High spatial resolution stress measurements using synchrotron based scanning X-ray microdiffraction with white or monochromatic beam. Materials Science & Engineering A: Structural Materials: Properties, Microstructure and Processing, 2005, 399, 92-98.	2.6	51
236	Multiscale Study of Internal Stress and Texture in Ferroelectrics. Materials Science Forum, 2005, 490-491, 28-28.	0.3	1
237	Application of the White/Monochromatic X-Ray μ-Diffraction Technique to the Study of Texture and Triaxial Strain at the Submicron Level. Materials Science Forum, 2005, 490-491, 672-677.	0.3	2
238	Synchrotron X-ray Micro-diffraction Analysis on Microstructure Evolution in Sn under Electromigration. Materials Research Society Symposia Proceedings, 2005, 863, B9.10-1.	0.1	4
239	Strain mapping on gold thin film buckling and silicon blistering. Materials Research Society Symposia Proceedings, 2005, 875, 1.	0.1	2
240	Microdiffraction Study of Polycrystalline Copper during Uniaxial Tension Deformation Using a Synchrotron X-Ray Source. Materials Science Forum, 2005, 475-479, 4149-4152.	0.3	0
241	Zinc mobility and speciation in soil covered by contaminated dredged sediment using micrometer-scale and bulk-averaging X-ray fluorescence, absorption and diffraction techniques. Geochimica Et Cosmochimica Acta, 2005, 69, 1173-1198.	1.6	89
242	Natural speciation of Mn, Ni, and Zn at the micrometer scale in a clayey paddy soil using X-ray fluorescence, absorption, and diffraction. Geochimica Et Cosmochimica Acta, 2005, 69, 4007-4034.	1.6	109
243	Electromigration-induced microstructure evolution in tin studied by synchrotron x-ray microdiffraction. Applied Physics Letters, 2004, 85, 2490-2492.	1.5	66
244	Shear at Twin Domain Boundaries inYBa2Cu3O7â [°] x. Physical Review Letters, 2004, 92, 216105.	2.9	8
245	X-ray Microdiffraction Characterization of Deformation Heterogeneities in BCC Crystals. Materials Research Society Symposia Proceedings, 2004, 840, Q7.2.1.	0.1	1
246	Coupling Between Precipitation and Plastic Deformation During Electromigration in a Passivated Al (0.5wt%Cu) Interconnect. Materials Research Society Symposia Proceedings, 2004, 812, F7.4.1.	0.1	0
247	In-situ Synchrotron X-ray Microdiffraction Study of Lattice Rotation in Polycrystalline Materials during Uniaxial Deformations. AIP Conference Proceedings, 2004, , .	0.3	0
248	In situ synchrotron X-ray microdiffraction study of deformation behavior in polycrystalline coppers during uniaxial deformations. Scripta Materialia, 2004, 51, 1183-1186.	2.6	11
249	Evidence of plastic damage in thin films around buckling structures. Thin Solid Films, 2004, 469-470, 221-226.	0.8	18
250	Quantitative characterization of electromigration-induced plastic deformation in Al(0.5wt%Cu) interconnect. Microelectronic Engineering, 2004, 75, 24-30.	1.1	16
251	X-ray microdiffraction: local stress distributions in polycrystalline and epitaxial thin films. Microelectronic Engineering, 2004, 75, 117-126.	1.1	21
252	Microstructure and superconductivity of MgB2 single crystals. Current Applied Physics, 2004, 4, 272-275.	1.1	6

#	Article	IF	CITATIONS
253	Natural speciation of Zn at the micrometer scale in a clayey soil using X-ray fluorescence, absorption, and diffraction. Geochimica Et Cosmochimica Acta, 2004, 68, 2467-2483.	1.6	156
254	Unexpected Mode of Plastic Deformation in Cu Damascene Lines Undergoing Electromigration. Materials Research Society Symposia Proceedings, 2004, 812, F7.3.1.	0.1	6
255	Tin whiskers studied by synchrotron radiation scanning X-ray micro-diffraction. Acta Materialia, 2003, 51, 6253-6261.	3.8	166
256	Twinning in La0.95Sr0.05Ga0.9Mg0.1O2.92crystal studied by white-beam (Laue) X-ray microdiffraction. Journal of Applied Crystallography, 2003, 36, 1197-1203.	1.9	13
257	Scanning X-ray microdiffraction with submicrometer white beam for strain/stress and orientation mapping in thin films. Journal of Synchrotron Radiation, 2003, 10, 137-143.	1.0	245
258	Direct measurement of triaxial strain fields around ferroelectric domains using X-ray microdiffraction. Nature Materials, 2003, 2, 379-381.	13.3	74
259	Molecular-Scale Speciation of Zn and Ni in Soil Ferromanganese Nodules from Loess Soils of the Mississippi Basin. Environmental Science & Technology, 2003, 37, 75-80.	4.6	171
260	X-ray microdiffraction study of growth modes and crystallographic tilts in oxide films on metal substrates. Nature Materials, 2003, 2, 487-492.	13.3	114
261	X-Ray absorption spectroscopy of transition metal–magnesium hydride thin films. Journal of Alloys and Compounds, 2003, 356-357, 204-207.	2.8	30
262	Workshop on Application of Xâ€ray Microdiffraction to Materials and Environmental Sciences. Synchrotron Radiation News, 2003, 16, 6-7.	0.2	0
263	Elastic Properties of Supported Polycrystalline Thin Films and Multilayers: an X-Ray Diffraction Study. Materials Science Forum, 2003, 426-432, 3409-3414.	0.3	0
264	Early stage of plastic deformation in thin films undergoing electromigration. Journal of Applied Physics, 2003, 94, 3757-3761.	1.1	55
265	Local Plasticity of Al Thin Films as Revealed by X-Ray Microdiffraction. Physical Review Letters, 2003, 90, 096102.	2.9	55
266	Mesoscale x-ray diffraction measurement of stress relaxation associated with buckling in compressed thin films. Applied Physics Letters, 2003, 83, 51-53.	1.5	23
267	Quantitative analysis of dislocation arrangements induced by electromigration in a passivated Alâ€,(0.5â€,wt %â€,Cu) interconnect. Journal of Applied Physics, 2003, 93, 5701-5706.	1.1	32
268	Quantitative Characterization of Dislocation Structure coupled with Electromigration in a Passivated Al (0.5wt%Cu) Interconnects. Materials Research Society Symposia Proceedings, 2003, 766, 121.	0.1	2
269	Electromigration-induced plastic deformation in passivated metal lines. Applied Physics Letters, 2002, 81, 4168-4170.	1.5	82
270	Microstructure and pinning properties of hexagonal-disc shaped single crystallineMgB2. Physical Review B, 2002, 66, .	1.1	19

#	Article	IF	CITATIONS
271	High spatial resolution grain orientation and strain mapping in thin films using polychromatic submicron x-ray diffraction. Applied Physics Letters, 2002, 80, 3724-3726.	1.5	85
272	Macro Stress Mapping on Thin Film Buckling. Materials Science Forum, 2002, 404-407, 709-714.	0.3	2
273	Deciphering Ni sequestration in soil ferromanganese nodules by combining X-ray fluorescence, absorption, and diffraction at micrometer scales of resolution. American Mineralogist, 2002, 87, 1494-1499.	0.9	102
274	Spatially Resolved Characterization of Electromigration-Induced Plastic Deformation in al (0.5WT%) Tj ETQq0 0	0 rgBT /Ov	verlock 10 Tf S
275	High resolution microdiffraction studies using synchrotron radiation. AIP Conference Proceedings, 2002, , .	0.3	4
276	Submicron x-ray diffraction and its applications to problems in materials and environmental science. Review of Scientific Instruments, 2002, 73, 1369-1372.	0.6	168
277	Trace metal fluxes to ferromanganese nodules from the western Baltic Sea as a record for long-term environmental changes. Chemical Geology, 2002, 182, 697-709.	1.4	51
278	Residual stress mapping by micro X-ray diffraction: Application to the study of thin film buckling. European Physical Journal Special Topics, 2002, 12, 409-416.	0.2	3
279	Quantitative Speciation of Heavy Metals in Soils and Sediments by Synchrotron X-ray Techniques. Reviews in Mineralogy and Geochemistry, 2002, 49, 341-428.	2.2	264
280	Local Microstructure and Stress in Al(Cu) Thin Film Structures Studied by X-Ray Microdiffraction. Materials Research Society Symposia Proceedings, 2001, 673, 1.	0.1	6
281	Submicron X-ray diffraction. Nuclear Instruments and Methods in Physics Research, Section A: Accelerators, Spectrometers, Detectors and Associated Equipment, 2001, 467-468, 936-943.	0.7	92
282	Grain Orientation and Strain Measurements in Sub-Micron wide Passivated Individual Aluminum Test Structures. Materials Research Society Symposia Proceedings, 2000, 612, 881.	0.1	10
283	Anomalous-X-ray scattering associated with short-range order in an Al70Ni15Co15 decagonal quasicrystal. Materials Science & Engineering A: Structural Materials: Properties, Microstructure and Processing, 2000, 294-296, 299-302.	2.6	11
284	Microtexture and Strain in Electroplated Copper Interconnects. Materials Research Society Symposia Proceedings, 2000, 612, 1031.	0.1	15
285	Isotropic magnetoresistance of icosahedral Al-Pd-Mn. Physical Review B, 1999, 60, 7208-7212.	1.1	18
286	A contribution to the Al–Pd–Mn phase diagram. Journal of Alloys and Compounds, 1999, 290, 164-171.	2.8	50
287	X-Ray Microbeam Measurement of Local Texture and Strain in Metals. Materials Research Society Symposia Proceedings, 1999, 563, 169.	0.1	18
288	Strain and Texture in Al-Interconnect Wires Weasured by X-Xay Microbeam Diffraction. Materials Research Society Symposia Proceedings, 1999, 563, 175.	0.1	32

#	Article	IF	CITATIONS
289	3-D Measurement of Deformation Microstructure in Al(0.2%)Mg Using Submicron Resolution White x-ray Microbeams. Materials Research Society Symposia Proceedings, 1999, 590, 247.	0.1	15
290	Atomic model of dislocations in Al-Pd-Mn icosahedral quasicrystals. Philosophical Magazine A: Physics of Condensed Matter, Structure, Defects and Mechanical Properties, 1998, 77, 1481-1497.	0.8	31
291	Effect of Rolling Direction on Recrystallization Behavior of Al-0.6 mass%Mg Alloy with Columnar Grains. Materials Transactions, JIM, 1998, 39, 334-342.	0.9	1
292	The concept of crystalline approximants for decagonal and icosahedral quasicrystals. Philosophical Magazine A: Physics of Condensed Matter, Structure, Defects and Mechanical Properties, 1997, 76, 337-356.	0.8	30
293	Selective ion sputtering and initial oxidation in Alî—,Pdî—,Mn single quasicrystals. Scripta Materialia, 1996, 35, 891-895.	2.6	24
294	Magnetic and transport properties of single grain AlPdMn quasicrystals. European Physical Journal D, 1996, 46, 2703-2704.	0.4	3
295	Diffusion ofMn54andFe59in icosahedral Al-Pd-Mn single quasicrystals. Physical Review B, 1996, 54, R6815-R6818.	1.1	49
296	Evidence for a Cluster-Based Structure of AlPdMn Single Quasicrystals. Physical Review Letters, 1996, 77, 3827-3830.	2.9	161
297	Triacontahedral growth morphology in icosahedral ZnMg-Y alloy. Philosophical Magazine Letters, 1996, 74, 89-98.	0.5	16
298	Monoclinic Al13Fe4 approximant phase: a link between icosahedral and decagonal phases. Journal of Non-Crystalline Solids, 1993, 153-154, 126-131.	1.5	37
299	Classification, based on energetics, of ideal icosahedral clusters, and building blocks of icosahedral quasicrystals and approximant crystals. Journal of Non-Crystalline Solids, 1993, 153-154, 546-551.	1.5	6
300	Structural Modelling of Quasicrystals. Key Engineering Materials, 1993, 81-83, 73-82.	0.4	0
301	High-resolution electron microscopy image simulations on the R-Al5CuLi3icosahedral approximant phase. Philosophical Magazine Letters, 1992, 65, 311-319.	0.5	3
302	Research of quasicrystalline state in TiNiV system. Phase Transitions, 1991, 32, 125-129.	0.6	3
303	Construction of 6D icosahedral crystals from approximate icosahedral 3D crystalline structures and phase transitions. Phase Transitions, 1991, 32, 89-101.	0.6	3
304	Structure and kinetics of Sn whisker growth on Pb-free solder finish. , 0, , .		33
305	Microstructure evolution of tin under electromigration studied by synchrotron x-ray micro-diffraction. , 0, , .		0
306	Synchrotron Radiation Based X-ray Micro-Diffraction Study on Reliability Issues of Solder Joints in Electronic Packaging Technology. , 0, , .		0